Desalination and Water Treatment
www.deswater.com
doi: 10.1080/19443994.2014.974213

57 (2016) 1659–1670
January

Taylor & Francis
Taylor & Francis Group

The enhancing effect of weak magnetic field on degradation of Orange II by zero-valent iron

Zhongjin Xiao, Qiaoli Zhou, Hejie Qin, Junlian Qiao*, Xiaohong Guan

State Key Laboratory of Pollution Control and Resources Reuse, Tongji University, Shanghai 200092, P.R. China, Tel. +86 021 65980025; emails: xiaozhongjinhit@163.com (Z. Xiao), zhouqiaoli2011@126.com (Q. Zhou), chinhj@foxmail.com (H. Qin), Tel. +86 021 65986313; email: qiaoqiao@tongji.edu.cn (J. Qiao), Tel. +86 021 65980956; email: guanxh@tongji.edu.cn (X. Guan)

Received 29 March 2014; Accepted 2 October 2014

ABSTRACT

The effects of weak magnetic field (WMF) on degrading Orange II by zero-valent iron (ZVI) as functions of pH_{ini}, ZVI dosages, and Orange II concentrations were investigated. The pseudo-first-order rate constants of Orange II removal by ZVI decreased progressively from 0.0057 to 0.0006 min^{-1} without WMF and from 0.0419 to 0.0039 min^{-1} with WMF, respectively, as pH_{ini} increased from 3.3 to 5.5. The pseudo-first-order rate constants of Orange II sequestration by ZVI were increased by 2.6- to 21-folds due to the application of WMF under the reaction conditions investigated in this study. The WMF-induced improvement in Orange II removal by ZVI was attributed to the accelerated corrosion of ZVI in the presence of WMF. The application of WMF not only improved the decolorization efficiency, but also enhanced TOC removal dramatically. The influence of radical scavenger and oxygen on Orange II removal as well as the FTIR analysis revealed that Orange II was removed via reduction by ZVI as well as adsorption/co-precipitation by the corrosion products. The method of employing WMF to enhance contaminants removal by ZVI is considered to be a promising technique in future water treatment since it does not need extra energy and costly reagents.

Keywords: Weak magnetic field; Zero-valent iron; Orange II; Degradation

1. Introduction

Azo dyes, widely used in the textile and dyestuff industries, account for almost half of all dye productions [1]. Orange II, one of the azo dyes, is widely used as coloring agent in a variety of product, such as paper, food stuffs, hair dye, and leather [2]. Orange II is known to be toxic, carcinogenic, mutagenic, and teratogenic, thus constitutes a significant burden on environment since Orange II has been applied illegally in a variety of industries, particularly in recent years [3–6]. Traditional physical methods such as flocculation, membrane, and adsorption only simply transfer the dyes from the liquid phase to the solid phase rather than destroying them [7,8]. Some chemical oxidation processes such as UV/H_2O_2, UV/O_3, UV/TiO_2, and the Fenton reaction have served to remove color and achieve mineralization effectively, yet are limited to the laboratory because of their rigorous operation conditions [9–13].

---

*Corresponding author.

During the past two decades, ZVI, as a readily available, inexpensive, nontoxic, and moderately strong reducing agent has been shown to decolorize the solution containing azo dyes and enhance its biodegradability [1,14]. Nam and Tratnyek [15] showed that nine kinds of azo dyes were rapidly decolorized by ZVI, which was due to the reduction of the azo groups and the formation of aromatics amines as products. Despite effective decolorization was achieved by ZVI alone, the mineralization rate was low due to the generation of organic intermediates, which require further treatment to meet the stringent effluent discharge standards. Moreover, ZVI is found to be deactivated over time due to the formation of iron oxides/hydroxides on the iron surface, which will hinder the further reaction of dyes with ZVI [16]. Therefore, many methods, including combing ultrasound with ZVI [17], UV/ZVI [18], nanoscale ZVI [19], iron–nickel bimetallic nanoparticle [20], ZVI/H_2O_2 [21], and ZVI-UV/H_2O_2 [22], have been developed to enhance the decolorization and mineralization rate of dyes by ZVI. However, the improvements induced by ultrasound or UV were minor, and extra chemicals were necessary for ZVI/H_2O_2 and ZVI-UV/H_2O_2 processes, which made the operation complicated and increased the operation cost. Although iron is inexpensive in bulk form, nanoscale ZVI and iron–nickel bimetal are much more expensive because the costly precursor reagents and complicated processes are needed to synthesize them [23]. Therefore, it is of urgent need to develop other inexpensive and highly efficient methods to improve dyes sequestration by ZVI.

Jiang et al. [24] reported that there was a 30–50% improvement in SO_2 absorption by cast iron scraps due to the application of DC magnetic field (10–20 mT), which may be associated with the increased ZVI corrosion rate facilitated by the looser corrosion products. Kim et al. [25] reported that the application of magnetic field ($\leq$ 40 mT) on the ZVI slurry markedly enhanced 4-chlorophenol removal from 26 to 54% under air-equilibrated condition, ascribed to the production of more $^{\cdot}OH$ radicals resulted from the easier transport of oxygen to ZVI surface in the presence of magnetic field. We observed that Se(IV) removal by ZVI was significantly improved by applying a weak magnetic field (WMF) ($B_{max} < 20$ mT) and showed that the external WMF could remarkably accelerate the corrosion of ZVI and lead to a faster release of Fe^{2+} [26]. According to the enhancing effects of magnetic field on Se(IV) removal by ZVI, it is expected that the dyes removal by ZVI can also be accelerated in the presence of WMF. However, up to now, no report on the WMF effects on dyes removal by ZVI is available. Therefore, this study was performed to examine the WMF effect on Orange II, one of the most widely used azo dyes in the textile industry, removal by ZVI. The objectives of this study were to (1) investigate the influence of WMF on the degradation of Orange II by ZVI as functions of initial solution pH levels, ZVI dosages, and Orange II concentrations; (2) explore the effect of WMF on the degradation mechanisms of Orange II; and (3) put a preliminarily light on the remarkable enhancement of WMF on Orange II removal by ZVI.

2. Materials and methods

2.1. Materials and chemicals

All chemicals were of analytical grade and used as received without any further purification. The ZVI powder with purity of >98% employed in our study was purchased from Sinopharm Chemical Reagent Co., Ltd. The median particle size and the specific surface area measured of this ZVI were 40 μm and 0.15 m^2/g, respectively. All the other chemicals employed in this study including Orange II, HCl, NaOH, and CH_3OH were also purchased from Sinopharm Chemical Reagent Co., Ltd. The chemical structure of Orange II is shown in Fig. 1. The stock solutions were prepared by dissolving the corresponding salts in ultrapure water generated from a Milli-Q water purification system.

2.2. Batch experiments

The experiments were carried out in a 1,000-mL beaker, which was placed in a water bath to control temperature constant at 25℃. The experiments were performed opened to the air, and the solution was mixed with a propeller-type stirrer at 450 r/min. With this stirring intensity, the aggregation of ZVI was avoided so that the influence of WMF on aggregation of ZVI could be excluded. Two pieces of neodymium–iron–boron permanent magnets on an iron sheet, as illustrated in Fig. 2(b), were employed to offer magnetic

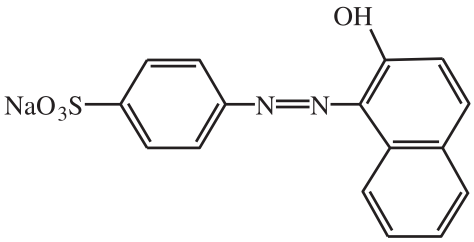

Fig. 1. The chemical structure of Orange II.

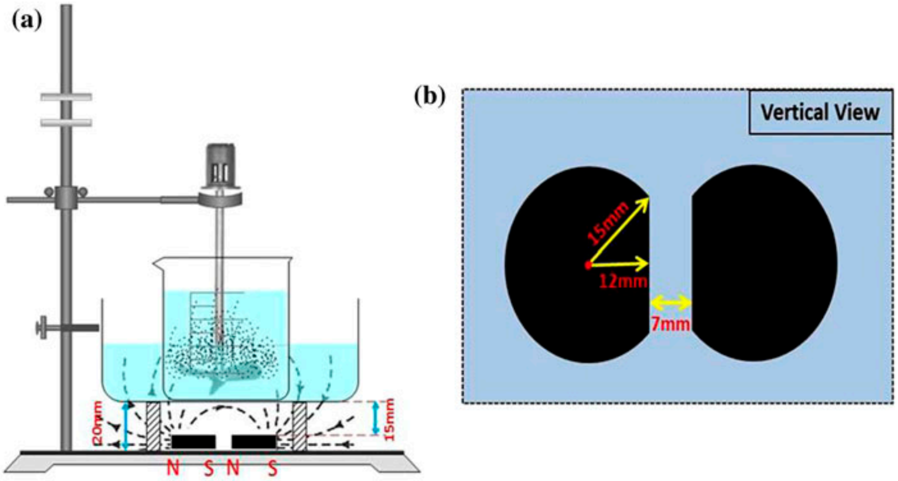

Fig. 2. (a) A laboratory-scale experimental set-up used in this experiment; (b) illustration of the size and layout of the two permanent magnets employed in this study. The N pole of one permanent magnet faces the S pole of the other.

field. The experimental set-up was schematically in Fig. 2(a), and the maximum magnetic field intensity was to be ~20 mT at the bottom of the reactor. The degradations of Orange II in coupled ZVI-WMF or ZVI alone system were investigated as functions of solution pH_{ini} levels (3.3–5.5), ZVI dosages (0.5–5 g/L), and initial Orange II concentration (25–150 mg/L). The pH_{ini} value of the solution was adjusted with 0.1 M HCl or 0.1 M NaOH, and it was not controlled during the reaction. The experiments were initiated by dosing ZVI of proper amount to Orange II-bearing solution.

The variation in solution pH value and the change in oxidation reduction potential (ORP) and the dissolved oxygen (DO) concentration were monitored during the degradation of Orange II at different pH_{ini} values with and without WMF. In addition, the effect of WMF on ZVI corrosion at different pH_{ini} values was also determined in the absence of Orange II. Furthermore, the influences of hydroxyl radical scavenger (CH_3OH) and dissolved O_2 on the removal of Orange II by ZVI were investigated. UV–Vis and FTIR analysis were employed to explore the degradation mechanisms and pathways of Orange II degradation by ZVI with and without WMF.

2.3. Chemical analyses

The concentration of Orange II was quantified by UV–Vis spectrophotometry (Beijing Puxi) at the λ_{max} = 484 nm, and UV–Vis spectra were collected from 200 to 600 nm. The measurements should be carried out as soon as possible after each sampling. Reaction solution was diluted five times before measurement to record spectra in most absorbance region, and the standard curve was modified according to the pH value of diluted reaction solution. FTIR spectra of pristine Orange II or ZVI powder reacted with Orange II solution were recorded as KBr pellets in the spectral range 4,000–400 cm^{-1} on a Perkin-Elmer 1725X FTIR spectrometer in air at room temperature. Total organic carbon (TOC) was monitored using a Shimadzu TOC analyzer (model TOC-V CPN, Japan) equipped with an auto-sampler to identify the mineralization of Orange II.

The solution pH value was detected by the pH meter (pHS-3C, Shanghai, China). The ORP was monitored with an ORP sensor connected to a pHS-3C pH meter. The concentration of DO was determined with a JPB-607A Portable Dissolved Oxygen Analyzer (Shanghai Precision & Scientific Instrument Co., Ltd). The intensity of magnetic field was determined by a Teslameter (HT201, Shanghai Hengtong Magnetic & Electric Technology Co., Ltd). Fe^{2+} concentration was examined by the modified ferrozine method using a TU-1901 UV/visible spectrophotometer at a wavelength of 562 nm [27]. All experiments were run in duplicates, all points in the figures are the mean of the results, and error bars represent standard deviation of the means.

3. Results and discussion

3.1. WMF effect on Orange II removal by ZVI at different initial pH levels

Fig. 3 reveals that the application of WMF significantly enhances the decolorization rate and efficiency

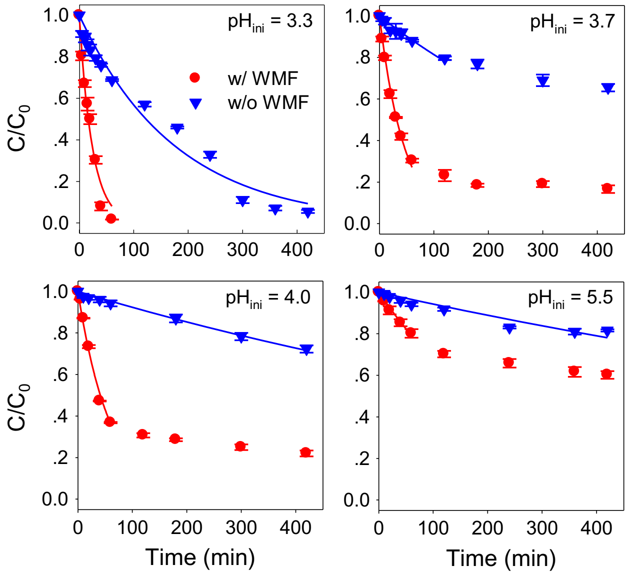

Fig. 3. Kinetics of Orange II removal by ZVI with and without WMF at different pH$_{ini}$ values. All data from stirred, open batch reactors with 2 g/L ZVI, 100 mg/L Orange II. Solid lines are fits to pseudo-first-order kinetics.

compared to their counterpart without WMF under the same reaction conditions. At pH$_{ini}$ 3.3, the decolorization efficiency reached approximately 100% within 60 min with WMF, while it took 7 h to obtain ~95% decolorization efficiency without WMF. The removal rates of Orange II by ZVI with and without WMF dropped with increasing pH$_{ini}$, but WMF consistently gives greater Orange II removal rate. The removal efficiencies of Orange II were enhanced from 35 to 84%, from 28 to 78%, and from 18 to 40%, respectively, at pH$_{ini}$ 3.7, 4, and 5.5, due to the application of WMF.

Pseudo-first-order kinetics was employed to simulate the kinetics of Orange II removal with and without WMF. It should be notified that only the kinetics data collected at the beginning of the reaction were employed to obtain the pseudo-first-order rate constants (k_{obs}) in case, the whole data set cannot be well described by pseudo-first-order kinetics. The fitting results are shown with solid lines in Fig. 3, and the obtained k_{obs} are summarized in Table 1.

Obviously, the decolorization rate of Orange II by ZVI was highly pH dependent regardless of the presence of WMF. Pseudo-first-order rate constants decreased progressively from 0.0057 to 0.0006 min^{-1} without WMF and from 0.0419 to 0.0039 min^{-1} with WMF, respectively, as pH$_{ini}$ increased from 3.3 to 5.5, indicating that the elevated pH was the primary cause for the decrease in rate and efficiency. The degradation of Orange II by ZVI is a heterogeneous process involving the oxidation and dissolution of iron in conjunction with the consumption of H$^+$ and release of Fe^{2+}. Thus, the favored degradation of Orange II by ZVI at lower pH should be mainly ascribed to the following reasons: (1) iron corrosion consumed H$^+$, as revealed by Eq. (1); (2) the interaction of negatively charged Orange II molecule with iron surface was facilitated at lower pH since the iron surface carry more positive charge at lower pH; (3) the lower pH should benefit the removal of the iron surface oxidation layer and then enhance the reaction on the surface of iron powder [28]. It was found that the rate constants of Orange II degradation by ZVI at different pH$_{ini}$ values were 7.4- to 21-folds greater with WMF than without. These amazing results revealed the outstanding advantage of WMF in improving ZVI reactivity toward Orange II removal and thus provided a

Table 1
Influence of WMF on the pseudo-first-order rate constants of Orange II removal by ZVI under different reaction conditions

			w/WMF		w/o WMF		
Orange II (mg/L)	ZVI (g/L)	pH$_{ini}$	k_1 (× 10^{-3} min^{-1})	r_1^2	k_2 (× 10^{-3} min^{-1})	r_2^2	k_1/k_2
100	2	3.3	41.9	0.97	5.7	0.97	7.35
100	2	3.7	21.8	0.99	2.1	0.92	10.38
100	2	4	16.8	0.99	0.8	0.98	21
100	2	5.5	3.9	0.97	0.6	0.91	6.50
100	0.5	3.3	6.7	0.91	1.4	0.94	4.79
100	1	3.3	10.1	0.87	2.6	0.89	3.88
100	2	3.3	41.9	0.97	5.7	0.97	7.35
100	5	3.3	115.2	0.96	20.1	0.97	5.73
25	2	3.3	183.6	0.99	24.2	0.99	7.59
50	2	3.3	81.2	0.95	9.3	0.96	8.73
100	2	3.3	41.9	0.97	5.7	0.97	7.35
150	2	3.3	13.7	0.94	5.2	0.94	2.63

new potential option to remove contaminants from wastewater more effectively.

$$Fe + O_2 + 2H^+ \rightarrow Fe^{2+} + H_2O \quad (1)$$

To further understand the influence of WMF on removal of Orange II by ZVI, the variation in solution pH value, the change in ORP and DO concentration at different pH_{ini} values in ZVI alone and coupled ZVI-WMF systems were monitored, and the results were shown in Fig. 4. The pH values of solution in both systems increased sharply after dosing ZVI into the Orange II solution, and the elevations in pH with WMF were always greater than that without WMF at different pH_{ini} values, implying that H^+ consumption was accompanied with Orange II removal by ZVI and thus increasing pH resulted in a decrease in Orange II removal rate. Moreover, the removal of Orange II resulted in a steep drop in DO concentration and ORP value. The drop in ORP at pH_{ini} 3.3–5.5 after the addition of ZVI may be ascribed to the decrease in DO and Orange II concentrations as well as the release of Fe^{2+} and the more significant drop with WMF than without should be mainly associated with the higher removal rate of Orange II, larger Fe^{2+} release rate, and oxygen consumption rate.

Due to the interference of color arising from Orange II, the concentration of Fe^{2+} generated in Orange II removal process was difficult to be detected by colorimetric method. Thus, the influence of WMF on ZVI corrosion at pH_{ini} 3.3 and 4 was investigated without the presence of Orange II, and the results are demonstrated in Fig. 5. Obviously, the application of WMF induced a sharper pH increase and ORP drop in the absence of Orange II, consistent with the trends obtained with Orange II. It was also confirmed that Fe^{2+} generation in the absence of Orange II was accelerated due to the application of WMF, implying that the WMF application accelerated ZVI corrosion and thus Orange II removal.

3.2. WMF effect on Orange II removal by ZVI as functions of iron dosages and Orange II concentrations

It is well known that the degradation reaction of organic compounds by ZVI is a kind of electrochemical reaction that occurs on the surface of iron metal, so the surface area of iron, determined by the dosage, should be of significance. Thus, the effect of WMF on decolorization rate of Orange II as a function of ZVI dosages was investigated, and the results are depicted in Fig. 6. Obviously, the decolorization rate of Orange II increased progressively with the increase in ZVI dosage with and without WMF.

When ZVI dosage was 0.5 g/L, the decolorization efficiencies with and without WMF were about 58% and 20% in 7 h, respectively. However, when the ZVI dosage was increased by 10-folds, almost complete decolorization was achieved within 20 min and 100 min, respectively, with and without WMF. As the ZVI dosage was elevated from 0.5 to 5 g/L, the pseudo-first-order rate constants of Orange II removal increased remarkably from 0.0014 to 0.0201 min^{-1} without WMF and from 0.0067 to 0.1152 min^{-1} with WMF. The rate constants of Orange II removal with WMF were 3.9- to 7.4-folds of those without WMF, indicating that the application of WMF could dramatically reduce the dosage of ZVI to achieve similar removal efficiency of contaminants.

The WMF influence on Orange II degradation was also investigated at different initial Orange II concentrations, and the results were illustrated in Fig. 7. The time necessary to achieve almost complete Orange II removal by ZVI without WMF was found to increase progressively with increasing initial Orange II concentration. Applying a WMF could considerably improve the removal rate of Orange II by ZVI, regardless of the initial Orange II concentration. When the initial concentration of Orange II was 50 mg/L, providing a WMF shortened the duration necessary to achieve almost complete decolorization from 240 to 30 min.

The reaction rate constant with and without WMF decreased from 0.1836 to 0.0137 min^{-1} and from 0.0242 to 0.0052 min^{-1}, respectively, when initial Orange II concentration increased from 25 to 150 mg/L. The drop in the rate constants of Orange II degradation with peroxymonosulfate catalyzed the magnetic cobalt nanoparticles anchored on graphene nanosheets and the $ZnFe_2O_4$-reduced graphene oxide hybrid were also reported [29,30]. Anyway, the removal rates of Orange II were accelerated by 2.6–8.7 times due to the presence of WMF at various initial Orange II concentrations.

3.3. WMF effect on decolorization and TOC removal

UV–Vis spectroscopy was applied to determine the formation of intermediates in the process of Orange II removal with and without WMF at different pH_{ini} values. UV–Vis spectra of Orange II solution recorded at given time intervals are presented in Fig. 8. The duration of collecting UV–Vis spectra lasted for 60 min at pH_{ini} 3.3, while for 180 min at other pH levels, regardless of the application of WMF.

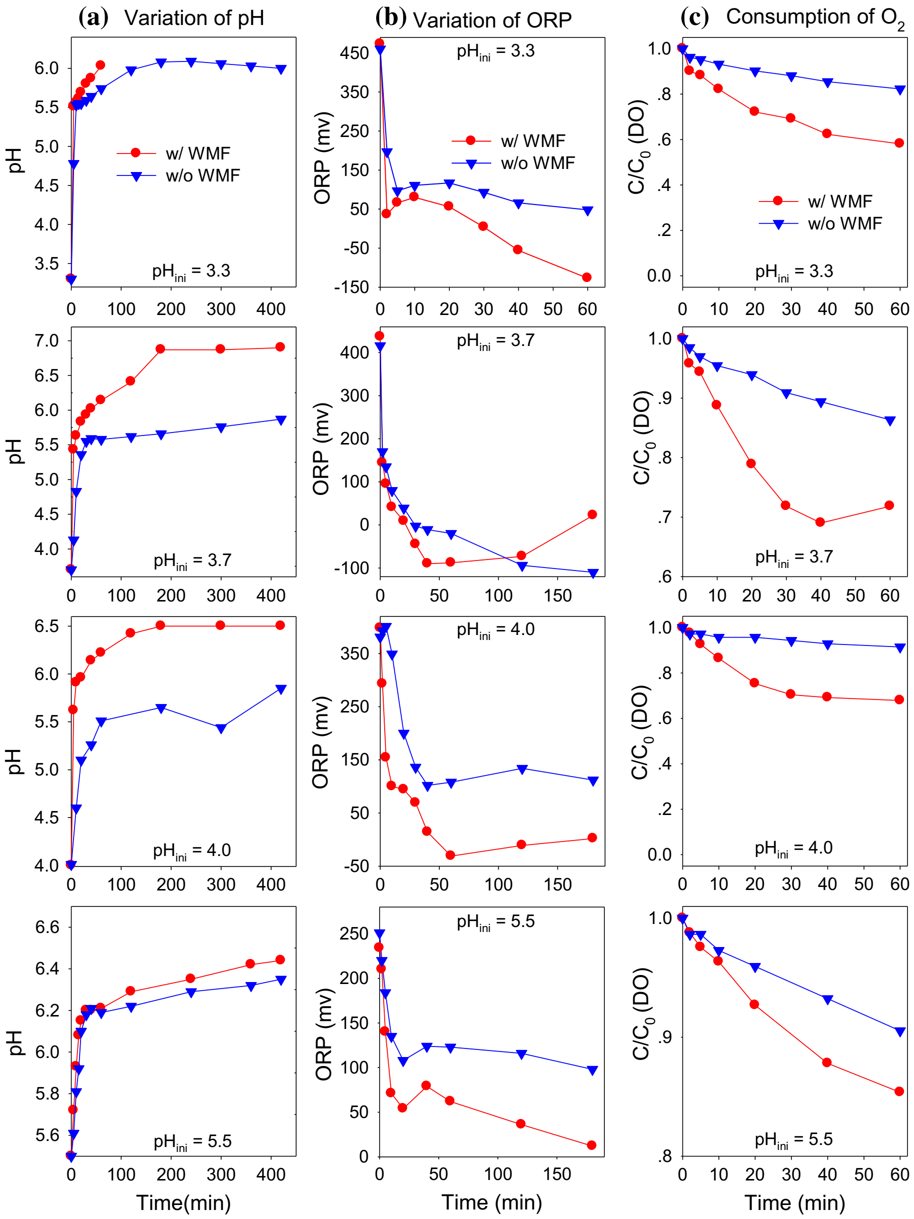

Fig. 4. Influence of WMF on variation in pH, ORP, and DO concentration at different pH_{ini} levels (reaction conditions: 100 mg/L Orange II, 2 g/L ZVI).

Orange II shows a strong absorbance band at 484 nm due to the n–π^* transition of –N=N– group. Other characteristic bands observed at 308 and 228 nm and the doublet at 261 and 254 nm can be assigned to π–π^* transition related to the aromatic rings of Orange II. Discoloration reaction took place by the vanishing of azo bond, evidenced by the decrease of the characteristic band at 484 nm. Fig. 8 illustrates that the variation trends of the characteristic bands of Orange II are very similar but with different rates except the case at pH_{ini} 3.3 with WMF. The dropping rate of the characteristic bands intensity decreased with increasing pH_{ini} with and without WMF, in accordance with the observations shown in Fig. 3. Moreover, the application of WMF resulted in a much stronger decrease in the intensity of characteristic bands at various pH levels. At pH_{ini} 3.3 with WMF, the disappearance of the characteristic bands at 484, 308, 261, 254, and 228 nm was accompanied with the appearance of a band at 250 nm, indicating the reduction of Orange II and the formation of 1-amino-2-naphthol as the major intermediate [31]. At other pH levels, the band at 250 nm was

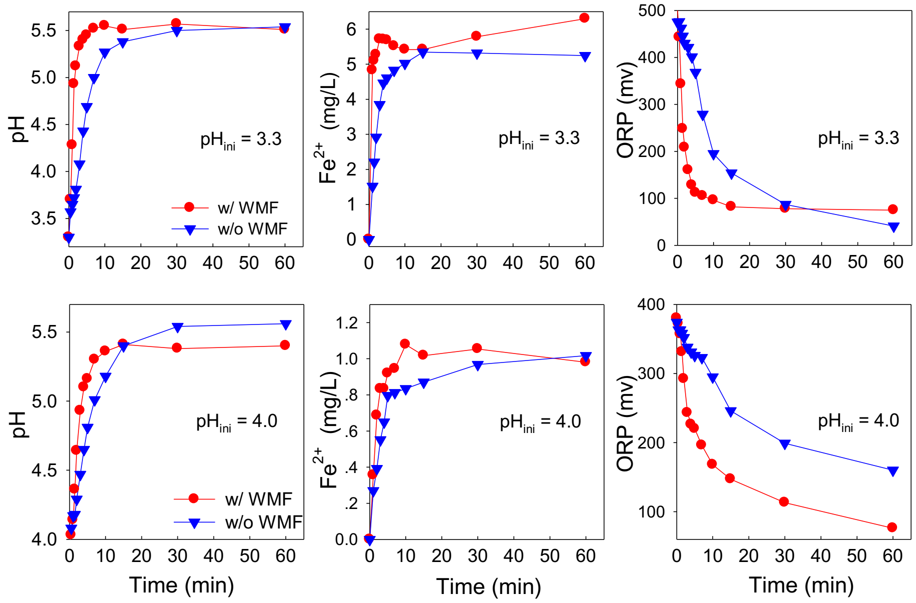

Fig. 5. Influence of WMF on variation in pH, accumulation of ferrous ion, variation in ORP at pH_{ini} 3.3 and pH_{ini} 4 (reaction conditions: 2 g/L ZVI, 100 mg/L Orange II).

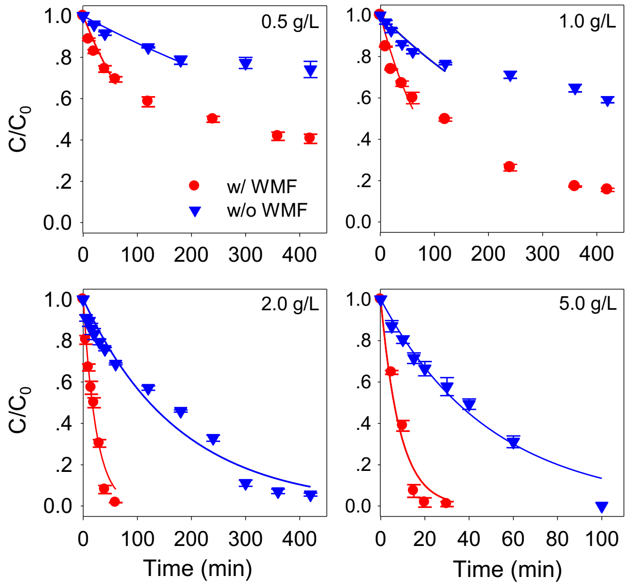

Fig. 6. Kinetics of Orange II removal by ZVI with and without WMF at different ZVI dosages. All data from stirred, open batch reactors with 100 mg/L Orange II and pH_{ini} 3.3. Solid lines are fits to pseudo-first-order kinetics.

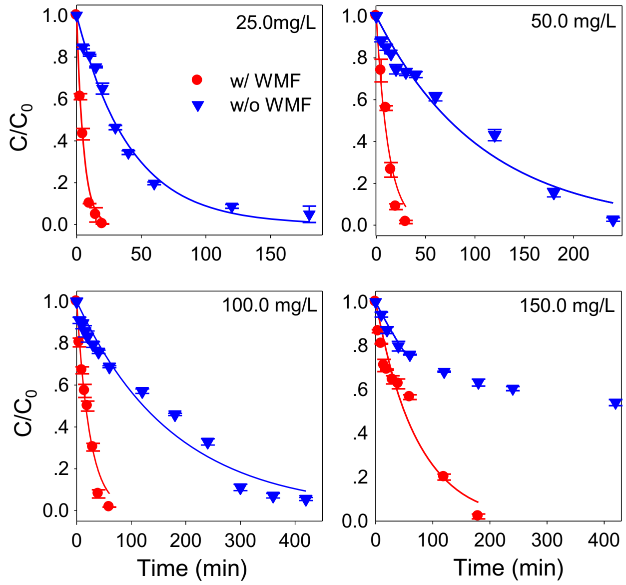

Fig. 7. Kinetics of Orange II removal by ZVI with and without WMF at different initial Orange II concentrations. All data from stirred, open batch reactors with 2 g/L ZVI and pH_{ini} 3.3. Solid lines are fits to pseudo-first-order kinetics.

not observed, which may be ascribed to the incomplete degradation of Orange II and the low content of 1-amino-2-naphthol formed in this process.

ZVI, as an electron donor, can lose electrons, and the Orange II molecule, as an electron acceptor, accepts electrons. Meanwhile, the dye molecule combines with H^+ and is transformed into the transitional products. These intermediate products also obtain electrons from ZVI and combine with H^+ again, after which they are transformed into terminal

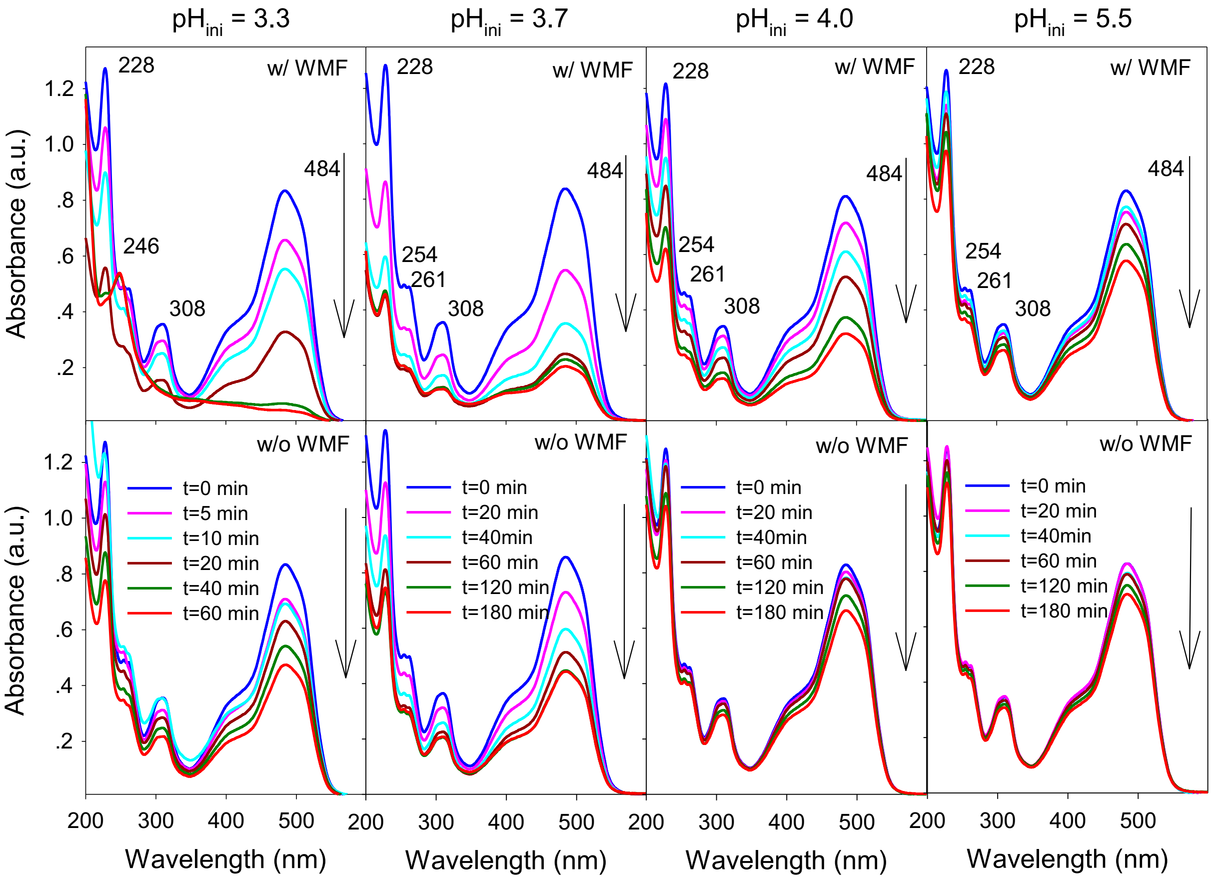

Fig. 8. Influence of WMF on UV–Vis spectrum changes at different pH_{ini} levels (reaction conditions: 100 mg/L Orange II, 2 g/L ZVI).

products such as sulfanilic acid and 1-amino-2-naphthol [15,31,32]. This process can be expressed with Eqs. (2)–(4).

$$Fe \rightarrow Fe^{2+} + 2e^- \tag{2}$$

$$NaO_3SC_6H_4\text{–}N = N\text{–}C_{10}H_6OH + 2e^- + 2H^+ \rightarrow NaO_3SC_6H_4\text{–}NH\text{–}NH\text{–}C_{10}H_6OH \tag{3}$$

$$NaO_3SC_6H_4\text{–}NH\text{–}NH\text{–}C_{10}H_6OH + 2e^- + 2H^+ \rightarrow NaO_3SC_6H_4\text{–}NH_2 + NH_2\text{–}C_{10}H_6OH \tag{4}$$

Decolorization and TOC removal are two major tasks in dye wastewater treatment. Despite effective decolorization can be generally achieved by ZVI reduction, the TOC removal is generally low, which limits the application of ZVI in dyes wastewater treatment. However, to our surprise, the application of WMF not only remarkably improved the decolorization efficiency, but also enhanced TOC removal dramatically. The TOC removal of Orange II solution at different pH_{ini} values, different ZVI dosages, and different Orange II concentrations with and without WMF after reaction for 3 h were investigated and shown in Fig. 9. The TOC removal without WMF was only significant at high ZVI dosage as well as low initial Orange II concentrations. However, the TOC removal with WMF was minor only when the pH_{ini} was 5.5 and the ZVI dosage was as low as 0.5 g/L and was as higher as 52–83% under other conditions investigated in this study. Thus, the application of WMF not only accelerated the decolorization of Orange II by ZVI but also remarkably enhanced the mineralization of Orange II.

3.4. *The mechanisms of the WMF-induced enhancement in Orange II removal*

Although many studies have been carried out on degrading Orange II by ZVI, there is still a debate on the mechanism of Orange II removal by ZVI. Some

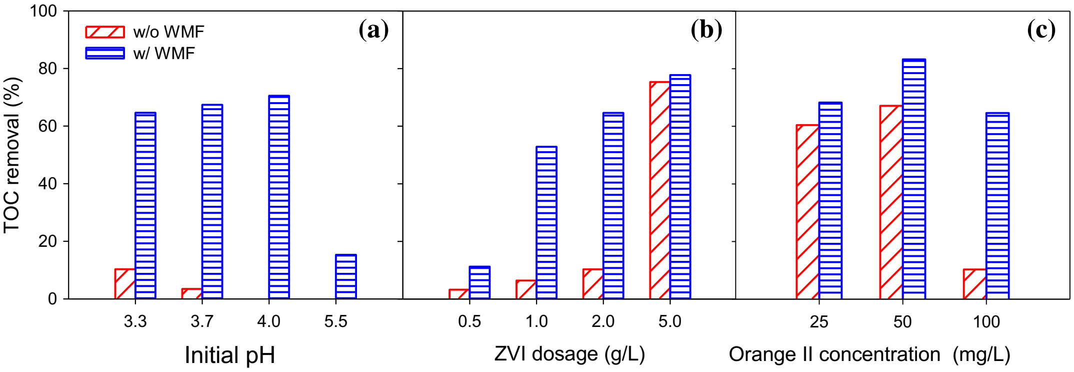

Fig. 9. Influence of WMF on mineralization of Orange II by ZVI under different reaction conditions. (a) 2 g/L ZVI, 100 mg/L Orange II; (b) pH_{ini} 3.3, 100 mg/L Orange II; and (c) pH_{ini} 3.3, 2 g/L ZVI.

argued that the removal of organic contaminants by ZVI was ascribed to reduction by ZVI and adsorption/co-precipitation by the corrosion products [28,33]. The formed passive iron oxides layers (Fe_3O_4, Fe_2O_3, $Fe(OH)_3$, and FeOOH) could adsorb dyes molecules via the sulfonic group and reduce the colority of the dye wastewater through the formation of a bridged bidentate complex [19]. However, other researchers declared that Fenton reaction, arising from the generation of Fe^{2+} and H_2O_2 in the process of ZVI corrosion open to the air, is responsible for the oxidative removal of dyes by ZVI [4].

In this study, all experiments were conducted open to the air, and thus, the ·OH scavenger was employed to verify the role of ·OH in Orange II removal by ZVI. Fig. 10 shows that the dosing of ·OH scavenger (CH_3OH) as high as 3.75 mol/L has little influence on the kinetics of Orange II with and without WMF, suggesting that the oxidation by ·OH contributes little to Orange II removal and Orange II may be mainly removed by reduction with ZVI. Therefore, influence of oxygen on Orange II degradation was examined and shown in Fig. 11.

Obviously, the removal of Orange II by ZVI with and without WMF was accelerated by purging the solution with N_2, implying that Orange II removal by ZVI was favored under anoxic condition. Thus, Orange II was most likely to be removed via reduction by ZVI as well as adsorption/co-precipitation by the corrosion products, which was further supported by the FTIR data, as illustrated in Fig. 12.

The intense absorption at 1,507 cm^{-1} in the FTIR spectrum of original Orange II is attributed to –N=N– bond vibrations, and the peaks at 1,121 and 1,037 cm^{-1} are due to the coupling between the benzene mode and $v_s(SO_3)$ [34]. The bands at 1,560 cm^{-1} and 1,453 cm^{-1} are linked to C=C aromatic skeletal vibrations and characteristic band of phenyl ring vibrations, respectively. The bands at 1,255 cm^{-1} and 1,205 cm^{-1} can be assigned to v(C–N) and v(N–N) stretching vibrations, respectively [35]. A strong peak at 1,023 cm^{-1}, arising from the generation of lepidocrocite, was observed in

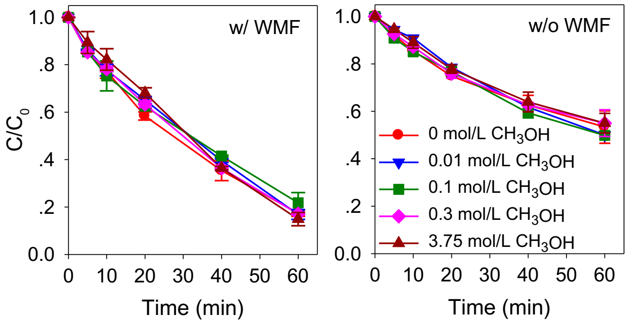

Fig. 10. Influence of hydroxyl radical scavenger (CH_3OH) on Orange II removal by ZVI. (reaction conditions: pH_{ini} 3.3, 2 g/L ZVI, 100 mg/L Orange II).

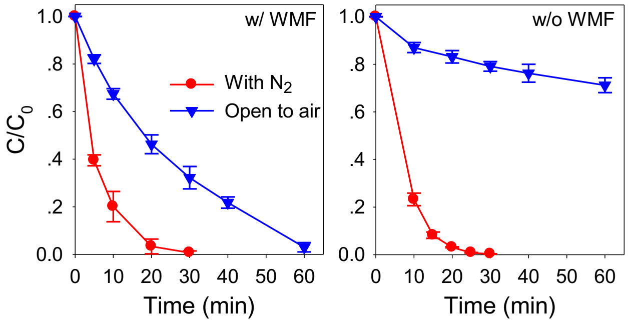

Fig. 11. The influence of DO on Orange II removal by ZVI. (reaction conditions: pH_{ini} 3.3, 2 g/L ZVI, 100 mg/L Orange II).

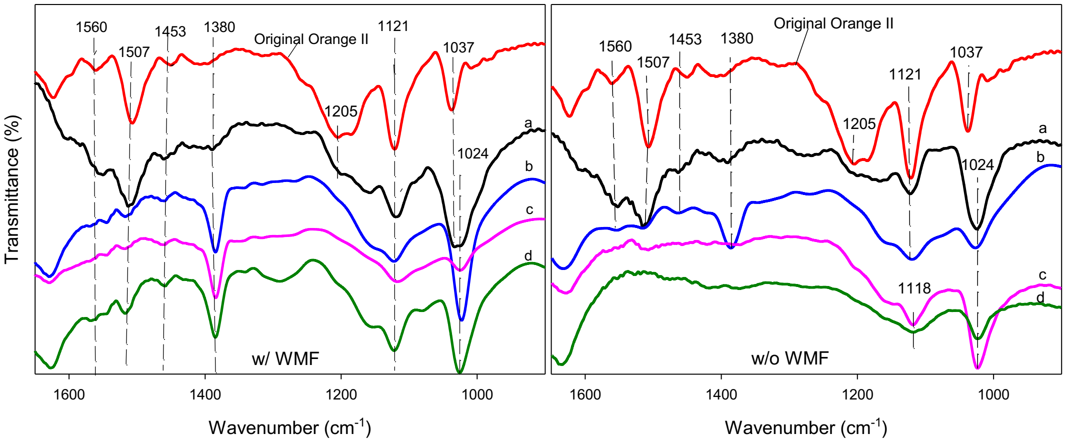

Fig. 12. Infrared analysis of original Orange II or ZVI particle reacted with Orange II with WMF or without WMF at different pH_{ini} values. (a) pH_{ini} 3.3, reaction time = 60 min; (b) pH_{ini} 3.7, reaction time = 180 min; (c) pH_{ini} 4, reaction time = 180 min; and (d) pH_{ini} 5.5, reaction time = 180 min (reaction conditions: 100 mg/L Orange II, 2 g/L ZVI).

the FTIR spectra of ZVI samples reacted with Orange II solution with and without WMF [31]. In addition, the intensity of the peak at 1,023 cm^{-1} in the FTIR spectra of ZVI samples with WMF was always stronger than its counterpart without WMF, implying the more intensive ZVI corrosion due to the application of WMF. The peaks at 1,507 cm^{-1}, 1,452 cm^{-1}, 1,380 cm^{-1}, and 1,121 cm^{-1}, which arise from either the parent Orange II compound or its degradation products, are observed in FTIR spectra of Orange II-treated ZVI samples at pH_{ini} 3.7–5.5 in the presence of WMF and those at pH_{ini} 3.3–3.7 in the absence of WMF. Therefore, Orange II and some intermediates are adsorbed or entrapped in the corrosion products of ZVI under these conditions. However, these bands are not observed in the ZVI samples treated with Orange II without WMF when the pH_{ini} is 4–5.5, which agrees with the non-removal of TOC under these conditions.

3.5. Discussion on the role of WMF in enhancing Orange II removal by ZVI

Based on the above results, it could be concluded that Orange II was removed by ZVI via reduction by ZVI and adsorption/co-precipitation by the corrosion products. The application of WMF accelerated the corrosion rate of ZVI and thus greatly improved Orange II removal by ZVI. Superimposing an inhomogeneous magnetic field to an electrochemical reaction introduced two body forces in the solution [36]. Firstly, a superposition of the dissolution current density (i) and the magnetic flux (B) results in the Lorentz force F_L

$$F_L = i \times B \tag{5}$$

It enhances the mass transfer by driving a macroscopic convection of the solution. As a result, the Lorentz force F_L induces a convective motion in the electrolyte and transports Fe^{2+} ions away from and H^+ toward the ZVI's surface [26]. Hence, the application of WMF facilitated the accumulation of H^+ on the ZVI's surface.

Secondly, due to the ferromagnetic nature of Fe, the metal becomes magnetized in the presence of magnetic fields which lead to an inhomogeneous flux density distribution in front of the Fe surface. In such an inhomogeneous magnetic field, the magnetic field gradient force F_B is

$$F_B = \chi m C \frac{B \nabla B}{\mu 0} \tag{6}$$

where χ_m is the molar magnetic susceptibility, μ_0 is the magnetic permeability of vacuum, and ∇B is the magnetic field gradient. F_B act on paramagnetic ions by pulling them into regions of high magnetic density and high magnetic field gradient since Fe^{2+} is paramagnetic, which result in uneven distribution of Fe^{2+} on the surface of Fe. Furthermore, the uneven distribution of Fe^{2+} will result in an uneven distribution of H^+ to preserve charge neutrality, which will result in extremely localized corrosion. Therefore, ZVI corrosion was accelerated by applying WMF, resulting in greater removal of Orange II with WMF than that without WMF.

4. Conclusion

In this study, the effects of WMF on degradation of Orange II by ZVI under different reaction conditions including different pH_{ini} levels, ZVI dosages, and Orange II concentrations were investigated. It was demonstrated that the application of WMF significantly improved the degradation efficiency and rate as well as TOC removal of Orange II by ZVI. The degradation kinetics of Orange II in the presence or absence of WMF was revealed to follow pseudo-first-order kinetics. The rate constants of Orange II removal by ZVI with and without WMF increased with decreasing pH_{ini} levels, increasing ZVI dosages, and decreasing initial Orange II concentrations. In our experiment, the degradation of Orange II by ZVI was demonstrated to be a reductive process rather than an oxidative process. UV–Vis spectra and FTIR spectra analysis indicated that the 1-amino-2-naphthol and sulfanilic acid were the major degradation products of Orange II. It also revealed that the removal of TOC of Orange II solution by ZVI was attributed to the adsorption/coprecipitation of Orange II or its degradation products by the ZVI corrosion products.

Acknowledgments

This work was supported by the National Natural Science Foundation of China (21277095, 51478329), and the Specialized Research Fund for the Doctoral Program of Higher Education (20130072110026).

References

[1] J.S. Cao, L.P. Wei, Q.G. Huang, L.S. Wang, S.K. Han, Reducing degradation of azo dye by zero-valent iron in aqueous solution, Chemosphere 38 (1999) 565–571.

[2] N. Pourreza, M. Zareian, Determination of Orange II in food samples after cloud point extraction using mixed micelles, J. Hazard. Mater. 165 (2009) 1124–1127.

[3] J. Zhan, G.Z. Fang, Z. Yan, M.F. Pan, C.C. Liu, S. Wang, Preparation of a semicovalent, molecularly surface imprinted polymer for the rapid determination of trace acid orange II in food and environmental samples, Anal. Bioanal. Chem. 405 (2013) 6353–6363.

[4] C. He, J.N. Yang, L.F. Zhu, Q. Zhang, W.C. Liao, S.K. Liu, Y. Liao, M. Abou Asi, D. Shu, pH-dependent degradation of acid orange II by zero-valent iron in presence of oxygen, Sep. Purif. Technol. 117 (2013) 59–68.

[5] H.Y. Li, Y.H. Gong, Q.Q. Huang, H. Zhang, Degradation of orange II by UV-assisted advanced fenton process: Response surface approach, degradation pathway, and biodegradability, Ind. Eng. Chem. Res. 52 (2013) 15560–15567.

[6] C.Q. Zhang, Z.W. Zhu, H.F. Zhang, Z.Q. Hu, Rapid decolorization of Acid Orange II aqueous solution by amorphous zero-valent iron, J. Environ. Sci. 24 (2012) 1021–1026.

[7] K. Dutta, S. Mukhopadhyay, S. Bhattacharjee, B. Chaudhuri, Chemical oxidation of methylene blue using a Fenton-like reaction, J. Hazard. Mater. 84 (2001) 57–71.

[8] L. Gomathi Devi, S. Girish Kumar, K. Mohan Reddy, C. Munikrishnappa, Effect of various inorganic anions on the degradation of Congo Red, a di azo dye, by the photo-assisted Fenton process using zero-valent metallic iron as a catalyst, Desalin. Water Treat. 4 (2009) 294–305.

[9] G. Ruppert, R. Bauer, G. Heisler, UV-O_3, UV-H_2O_2, UV-TiO_2 and the photo-Fenton reaction—Comparison of advanced oxidation processes for wastewater treatment, Chemosphere 28 (1994) 1447–1454.

[10] H.Y. Shu, C.R. Huang, Degradation of commercial azo dyes in water using ozonation and UV enhanced ozonation process, Chemosphere 31 (1995) 3813–3825.

[11] R.R. Ozer, J.L. Ferry, Investigation of the photocatalytic activity of TiO_2−polyoxometalate systems, Environ. Sci. Technol. 35 (2001) 3242–3246.

[12] M. Muruganandham, M. Swaminathan, Photochemical oxidation of reactive azo dye with UV-H_2O_2 process, Dyes Pigm. 62 (2004) 269–275.

[13] J.X. Chen, L.Z. Zhu, Heterogeneous UV-Fenton catalytic degradation of dyestuff in water with hydroxyl-Fe pillared bentonite, Catal. Today 126 (2007) 463–470.

[14] J.R. Perey, P.C. Chiu, C.P. Huang, D.K. Cha, Zero-valent iron pretreatment for enhancing the biodegradability of azo dyes, Water Environ. Res. 74 (2002) 221–225.

[15] S. Nam, P.G. Tratnyek, Reduction of azo dyes with zero-valent iron, Water Res. 34 (2000) 1837–1845.

[16] C.B. Wang, W.X. Zhang, Synthesizing nanoscale iron particles for rapid and complete dechlorination of TCE and PCBs, Environ. Sci. Technol. 31 (1997) 2154–2156.

[17] H. Zhang, L.J. Duan, Y. Zhang, F. Wu, The use of ultrasound to enhance the decolorization of the C.I. Acid Orange 7 by zero-valent iron, Dyes Pigm. 65 (2005) 39–43.

[18] N. Deng, F. Luo, F. Wu, M. Xiao, X. Wu, Discoloration of aqueous reactive dye solutions in the UV/Fe^0 system, Water Res. 34 (2000) 2408–2411.

[19] J. Fan, Y.H. Guo, J.J. Wang, M.H. Fan, Rapid decolorization of azo dye methyl orange in aqueous solution by nanoscale zerovalent iron particles, J. Hazard. Mater. 166 (2009) 904–910.

[20] A.D. Bokare, R.C. Chikate, C.V. Rode, K.M. Paknikar, Iron–nickel bimetallic nanoparticles for reductive degradation of azo dye Orange G in aqueous solution, Appl. Catal., B 79 (2008) 270–278.

[21] B.H. Moon, Y.B. Park, K.H. Park, Fenton oxidation of Orange II by pre-reduction using nanoscale zero-valent iron, Desalination 268 (2011) 249–252.

[22] M.C. Chang, H.Y. Shu, H.H. Yu, An integrated technique using zero-valent iron and UV/H_2O_2 sequential process for complete decolorization and mineralization of C.I. Acid Black 24 wastewater, J. Hazard. Mater. 138 (2006) 574–581.

[23] R.A. Crane, T.B. Scott, Nanoscale zero-valent iron: Future prospects for an emerging water treatment technology, J. Hazard. Mater. 211-212 (2012) 112–125.

[24] J.H. Jiang, Y.H. Li, W.M. Cai, Experimental and mechanism research of SO_2 removal by cast iron scraps in a magnetically fixed bed, J. Hazard. Mater. 153 (2008) 508–513.

[25] D.H. Kim, J. Kim, W. Choi, Effect of magnetic field on the zero valent iron induced oxidation reaction, J. Hazard. Mater. 192 (2011) 928–931.

[26] L.P. Liang, W. Sun, X.H. Guan, Y.Y. Huang, W. Choi, H.L. Bao, L.N. Li, Z. Jiang, Weak magnetic field significantly enhances selenite removal kinetics by zero valent iron, Water Res. 49 (2014) 371–380.

[27] X.H. Guan, H.R. Dong, J. Ma, I.M.C. Lo, X.M. Dou, Performance and mechanism of simultaneous removal of chromium and arsenate by Fe(II) from contaminated groundwater, Sep. Purif. Technol. 80 (2011) 179–185.

[28] M.F. Hou, F.B. Li, X.M. Liu, X.G. Wang, H.F. Wan, The effect of substituent groups on the reductive degradation of azo dyes by zerovalent iron, J. Hazard. Mater. 145 (2007) 305–314.

[29] Y.J. Yao, C. Xu, J.C. Qin, F.Y. Wei, M.N. Rao, S.B. Wang, Synthesis of magnetic cobalt nanoparticles anchored on graphene nanosheets and catalytic decomposition of orange II, Ind. Eng. Chem. Res. 52 (2013) 17341–17350.

[30] Y.J. Yao, J.C. Qin, Y.M. Cai, F.Y. Wei, F. Lu, S.B. Wang, Facile synthesis of magnetic $ZnFe_2O_4$-reduced graphene oxide hybrid and its photo-Fenton-like behavior under visible iradiation, Environ. Sci. Pollut. Res. 21 (2014) 7296–7306.

[31] J.A. Mielczarski, G.M. Atenas, E. Mielczarski, Role of iron surface oxidation layers in decomposition of azo-dye water pollutants in weak acidic solutions, Appl. Catal., B 56 (2005) 289–303.

[32] S. Luo, P.F. Qin, J.H. Shao, L. Peng, Q.R. Zeng, J.D. Gu, Synthesis of reactive nanoscale zero valent iron using rectorite supports and its application for Orange II removal, Chem. Eng. J. 223 (2013) 1–7.

[33] L.J. Matheson, P.G. Tratnyek, Reductive dehalogenation of chlorinated methanes by iron metal, Environ. Sci. Technol. 28 (1994) 2045–2053.

[34] M. Stylidi, D.I. Kondarides, X.E. Verykios, Pathways of solar light-induced photocatalytic degradation of azo dyes in aqueous TiO_2 suspensions, Appl. Catal., B 40 (2003) 271–286.

[35] G.S. Zhang, J.H. Qu, H.J. Liu, A.T. Cooper, R.C. Wu, $CuFe_2O_4$/activated carbon composite: A novel magnetic adsorbent for the removal of acid orange II and catalytic regeneration, Chemosphere 68 (2007) 1058–1066.

[36] R. Sueptitz, K. Tschulik, M. Uhlemann, L. Schultz, A. Gebert, Effect of high gradient magnetic fields on the anodic behaviour and localized corrosion of iron in sulphuric acid solutions, Corros. Sci. 53 (2011) 3222–3230.